Furrow-and-ridge morphology on rockglaciers explained by gravity-driven buckle folding: A case study from the Murtèl rockglacier (Switzerland)

Marcel Frehner[1], Isabelle Gärtner-Roer[2], and Anna H.M. Ling[1,2]

[1]Geological Institute, ETH Zurich, Switzerland, marcel.frehner@erdw.ethz.ch
[2]Department of Geography, University of Zurich, Switzerland

Summary

Our study promotes buckle folding as the dominant process for the formation of furrow-and-ridge morphology on rockglaciers. Applying analytical buckle folding expressions to a high-resolution digital elevation model of the Murtèl rockglacier allows us to estimate the viscosity ratio between the higher-viscous active layer and its almost pure ice substratum. Using these constraints in a dynamic finite-element model of viscous rockglacier flow reproduces all key natural observations of the furrow-and-ridge morphology.

1. Introduction

Rockglaciers often feature a prominent furrow-and-ridge morphology, for which the Murtèl rockglacier in Switzerland (Figure 1) is a spectacular example. Previous studies suggesting that a longitudinal compressive flow in the lower part of a rockglacier is responsible for these structures are based on qualitative descriptions and remained speculative.

Buckle folding is the mechanical response of a layered viscous material to shortening if the mechanical contrast between the layers is significant. The resulting buckle folds are common structures in rocks and are well-studied in field outcrops, experimentally, numerically, and mathematically.

We propose that gravity-driven buckle folding is also the main responsible process for the formation of the transverse furrow-and-ridge morphology on rockglaciers. In this cross-disciplinary study we use the buckle folding theory, which is well-established in the field of structural geology, and apply it to the field of rockglacier geomorphology.

2. Data and Methods

For building a representative model we require two key ingredients: accurate geometrical information and information on the material behavior (i.e., rheology). Both ingredients are elucidated below in two subchapters.

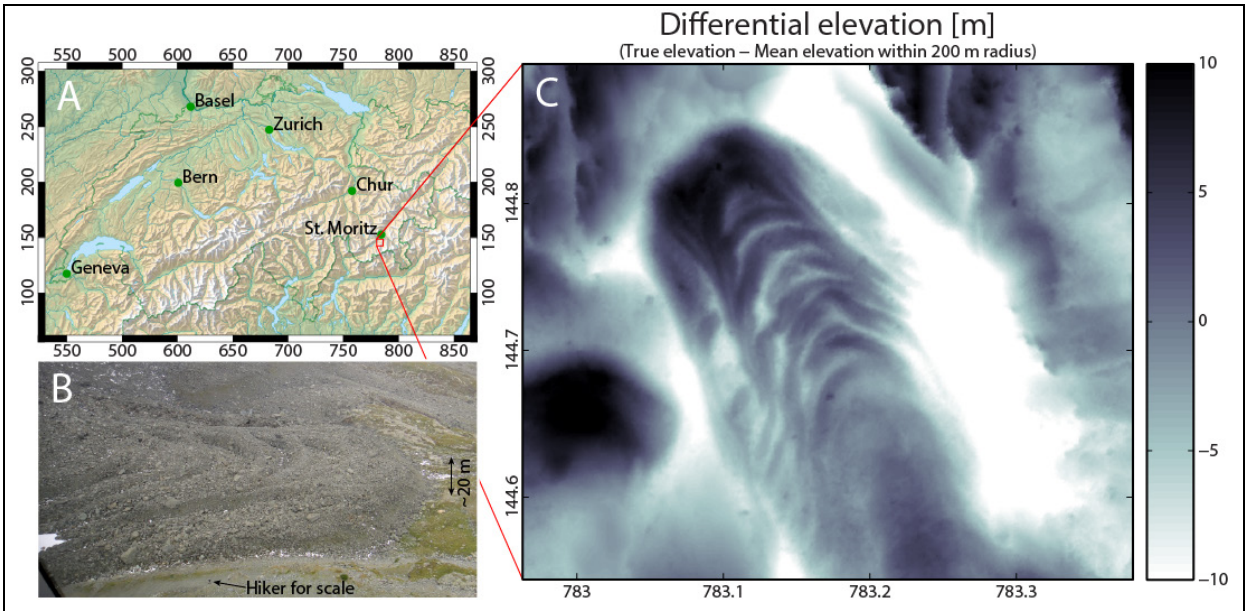

Figure 1: Location (A; source Swiss Federal Office of Topography) and surface structure (B, C) of the Murtèl rockglacier in Switzerland. The differential elevation is calculated as the true elevation minus the mean elevation within a 200 m diameter circle. The employed 1 m-resolution DEM is based on photogrammetry. Coordinates in Swiss coordinate system CH1903.

Geometrical Information

We analyze the surface topography using a 1 m-resolution digital elevation model (DEM) based on low-altitude aerial photographs. The three-dimensional (3D) furrow-and-ridge morphology is evident when considering the 200 m-diameter differential elevation (diffDEM; Figure 1C). The average wavelength of the furrow-and-ridge structure is around 20 m; the average amplitude is around 2 m.

Borehole deformation measurements (Arenson et al., 2002) demonstrate that the lower part of the Murtèl rockglacier is immobile and detached from the upper 30 m by a discrete shear zone. Borehole image logs and integrated interpretations of geoelectric, seismic, and georadar data (Maurer and Hauck, 2007) suggest that the upper part is relatively homogeneous and consists of almost pure ice. The top-most active layer is 3–5 m thick and is a mixture of ice and rock fragments with sizes from sand to boulders (Figure 1B), which freezes and unfreezes during the course of a year. Kääb et al. (1998) speculated that the thickness of the active layer below ridges is larger than below furrows.

Based on this geometrical information we approximate the Murtèl rockglacier as a two-layer system consisting of a lower 27 m thick layer and an upper 3–5 m thick layer. Both layers are assumed to obey a viscous flow law, the upper exhibiting a higher viscosity because of its rock fragment content. We consider the part below 30 m not important for the formation of furrows and ridges and we neglect it.

Rheological information

Borehole deformation experiments (Arenson et al., 2002) demonstrate that the shear zone at 30 m depth accommodates 60% of the total deformation. The parabolic flow profiles above the shear zone can be approximated using a viscous flow law. For the active layer it is not possible to determine the power-law exponent, first because it is a complex mixture of ice and rock fragments and second because the borehole data is too sparse in this layer. Hence, we treat both layers as Newtonian (linear viscous) materials. This assumption has the advantage that the modeled deformation does not depend on strain rate and on absolute viscosity values, but only on the viscosity ratio.

To determine the viscosity ratio, R, we assume that the furrow-and-ridge morphology is a result of viscous buckle folding. The Fold Geometry Toolbox (FGT; Adamuszek et al., 2011) automatically analyzes the geometry of a folded layer and applies various buckle folding theories to determine the viscosity ratio between the folded layer and its surrounding. We feed the FGT with longitudinal sections of the furrow-and-ridge geometry derived from the diffDEM (Figure 1C). We vary the thickness of the active layer (3–5 m; Figure 2A) according to its uncertainty and also use a non-constant thickness (Kääb et al., 1998). The FGT yields viscosity ratios of R=9–21 depending on the input model (Figure 2B).

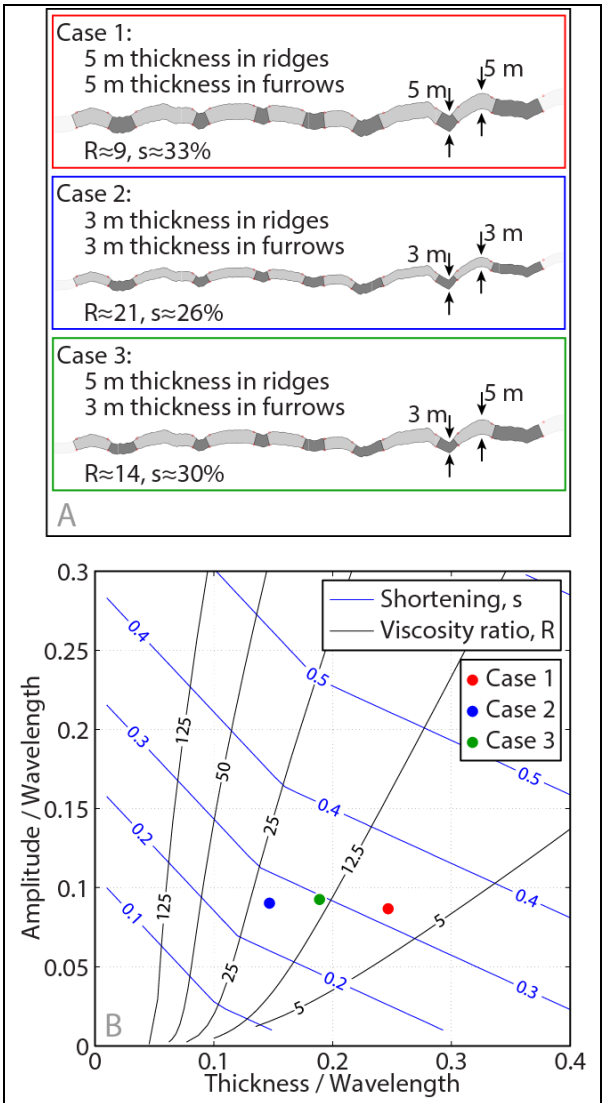

Figure 2: Geometrical and rheological information of the Murtèl rockglacier (modified screenshots from the FGT). A: Different input models using different layer thicknesses of the active layer. Gray shades: furrows and ridges as identified by the FGT. B: Resulting fold amplitude-to-wavelength and thickness-to-wavelength ratios with overlain shortening and viscosity ratio contour lines.

Numerical Finite-Element Modeling

Based on the above geometrical and rheological analysis we designed a finite-element (FE) model (Figure 3B) to simulate rockglacier flow under the effect of gravity. The model solves the governing force balance and rheological (Newtonian) equations in 2D (details in Frehner, 2011; Frehner et al., 2012). For the Murtèl rockglacier the 2D approximation is justified because of its straight tongue-like geometry and unidirectional flow field (Kääb et al., 1998). The initial model surface is randomly disturbed (Figure 3A), representing natural irregularities of rock fragments and boulders, but also allowing the mechanical buckling instability to initialize.

3. Results

Figure 3C and 4A show the initial model state. Because we only consider the viscosity ratio, calculated stresses cannot be taken as absolute stress levels. The active layer exhibits layer-parallel compression towards the rockglacier toe, which is also reflected by the orientation of the most compressive stress parallel to the layer. Immediately below the active layer, compression is much smaller but still layer-parallel. These discontinuous stresses across the layer interface drive the buckling instability.

For further analysis we focus on the rockglacier toe (Figure 4), where active buckling takes place. The modeled buckle folds develop self-consistently with a wavelength of around 20 m. Around 150 m from the rockglacier front, compression in the active layer is largest; hence buckle folds develop the fastest. Further towards the front, buckle folds still develop, but at a lower rate. This is directly comparable to the Murtèl rockglacier (Figure 1C). The amplitudes in Figure 4C of about 2 m are comparable to the present-day amplitudes on the Murtèl rockglacier; hence, Figure 4C represents today's situation while Figure 4B represents an earlier situation.

Figure 4D shows the modeled borehole deformation (colored lines) from the surface down to 5 m above the fixed model bottom. The deformation of all boreholes and for both time intervals exhibits the typical parabolic shape, confirming the viscous flow profile within the rockglacier. The developing buckle folds disturb this otherwise smooth deformation profile in the active layer. Naturally, data measured on the Murtèl rockglacier (gray lines) show more variations. However, on average the deformation profiles are also parabolic and disturbed in the active layer. Hence, the modeled borehole deformation profiles can be directly compared to the real data.

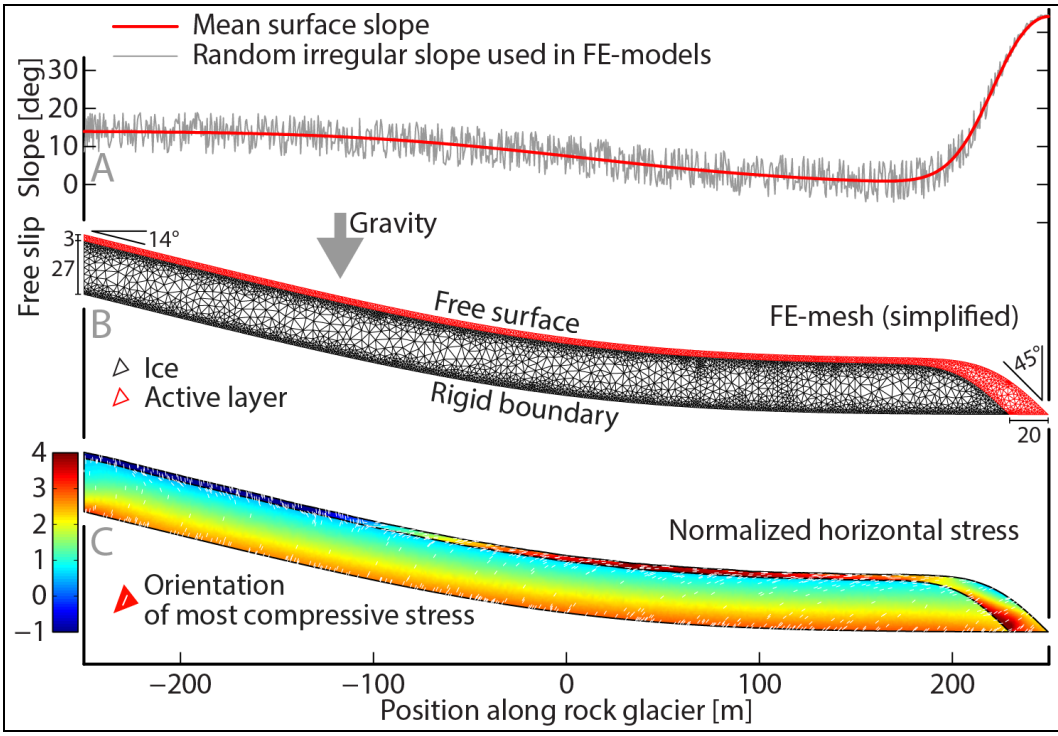

Figure 3: Initial and boundary conditions of the FE model, which is inspired by the Murtèl rockglacier. The numerical mesh (B) is simplified because the real mesh is too dense to be depicted. C shows the initial normalized horizontal stress (positive = compression) and the orientation of the most compressive stress as white lines.

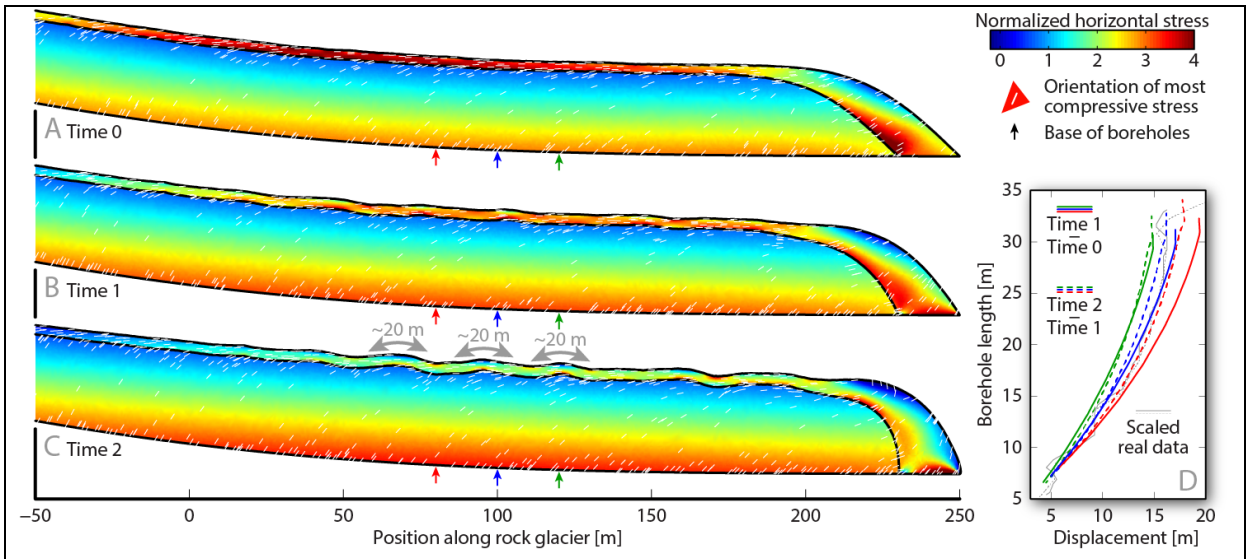

Figure 4: A–C: Snapshots at three different times (Times 0–2) of the rockglacier toe. D shows the modeled borehole deformation between Times 0 and 1 and between Times 1 and 2 at locations indicated in A–C. The two gray lines correspond to the borehole deformation data of Arenson et al. (2002) measured on the Murtèl rockglacier in a similar location.

4. Discussion

Because we do not accurately describe the shear zone, our FE simulation only accounts for 40% of the total deformation. Borehole deformation data and photogrammetric and terrestrial geodetic surveys yield surface velocities of the Murtèl rockglacier of 5 (Kääb et al., 1998) to 6 cm a^{-1} (Arenson et al., 2002; Müller et al., 2014). With 40% of this surface velocity, 625–950 years are necessary to reach the modeled surface displacement of 15–19 m (Figure 4D). While the natural 3D deformation (compared to the 2D model) may not significantly alter the deformation geometry, it does affect the rate of deformation. The curved furrows and ridges (Figure 1C) indicate a viscous flow pattern also in map-view resembling an open-channel flow. We estimate the velocity reduction in such a 3D flow to about 35% compared to our modeled 2D flow. Hence, the estimated time to develop the furrows and ridges extends to 960–1460 years. Time 1 in Figure 4 corresponds to 480–730 years and Time 2 corresponds to 960–1460 years after the initial state (Time 0).

5. Conclusions

Using the Murtèl rockglacier as an example, we promote gravity-driven viscous buckle folding as the dominant process explaining the furrow-and-ridge morphology characteristic for many rockglaciers. Buckle folding requires two main ingredients: mechanical layering and layer-parallel compression. In rockglaciers, the first is due to a layered ratio between ice and rock fragments. The second is due to the convex curvature of a rockglacier towards it toe. The associated slow-down leads to a compressive flow where curvature is largest. Our dynamical gravity-driven FE-model explains several first-order features of the Murtèl rockglacier: the amplitudes and wavelengths of the furrow-and-ridge morphology, the location of the largest-amplitude structures, and the parabolic flow profiles measured in boreholes. We estimate the time necessary to develop a furrow-and-ridge morphology as observed on the Murtèl rockglacier to be less than 1500 years.

References

Adamuszek, M., Schmid, D.W, and Dabrowski, M., 2011: Fold geometry toolbox – automated determination of fold shape, shortening, and material properties, Journal of Structural Geology, 33, 1406–1416.

Arenson, L., Hoelzle, M., and Springman, S., 2002: Borehole deformation measurements and internal structure of some rock glaciers in Switzerland, Permafrost and Periglacial Processes, 13, 117–135.

Frehner, M., 2011: The neutral lines in buckle folds, Journal of Structural Geology, 33, 1501–1508.

Frehner, M., Reif, D., and Grasemann, B., 2012: Mechanical versus kinematical shortening reconstructions of the Zagros High Folded Zone (Kurdistan Region of Iraq), Tectonics, 31, TC3002.

Kääb, A., Gudmundsson, G.H., and Hoelzle, M., 1998: Surface deformation of creeping mountain permafrost. Photogrammetric investigations on rock glacier Murtèl, Swiss Alps, Collection Nordicana, 55, 531–537.

Maurer, H. and Hauck, C., 2007: Instruments and methods geophysical imaging of alpine rock glaciers, Journal of Glaciology, 53, 110–120.

Müller, J., Gärtner-Roer, I., Kenner, R., Thee, P., and Marche, D. 2014: Sediment storage and transfer on a periglacial mountain slope (Corvatsch, Switzerland), Geomorphology, in press.